HHS Public Access

Author manuscript

Prostate. Author manuscript; available in PMC 2017 August 01.

Published in final edited form as:

Prostate. 2016 August ; 76(11): 964–976. doi:10.1002/pros.23185.

Obesity-initiated metabolic syndrome promotes urinary voiding dysfunction in a mouse model

Qiqi He[1,2], **Melissa A. Babcook**[1], **Sanjeev Shukla**[1], **Eswar Shankar**[1], **Zhiping Wang**[2], **Guiming Liu**[3], **Bernadette O. Erokwu**[4], **Chris A. Flask**[4,5,6], **Lan Lu**[1,4], **Firouz Daneshgari**[3], **Gregory T. MacLennan**[7], and **Sanjay Gupta**[1]

[1]Department of Urology, Case Western Reserve University & University Hospitals Case Medical Center, Cleveland, Ohio 44106

[2]Department of Urology, Key Laboratory of Disease of Urological Systems, Gansu Nephro-Urological Clinical Center, Second Hospital of Lanzhou University, Lanzhou, Gansu, China

[3]Department of Surgery, MetroHealth Medical Center, Case Western Reserve University, Cleveland, Ohio 44109

[4]Department of Radiology, Case Western Reserve University & University Hospitals Case Medical Center, Cleveland, Ohio 44106

[5]Department of Biomedical Engineering, Case Western Reserve University, Cleveland, Ohio 44106

[6]Department of Pediatrics, Case Western Reserve University & University Hospitals Case Medical Center, Cleveland, Ohio 44106

[7]Department of Pathology, Case Western Reserve University & University Hospitals Case Medical Center, Cleveland, Ohio 44106

Abstract

OBJECTIVE—Accumulating evidences suggests that obesity and metabolic syndrome (MetS) contribute towards lower urinary tract symptoms (LUTS) through alterations in the phenotype of bladder and prostate gland. Clinical studies indicate a link between MetS and LUTS. Nevertheless, there is lack of suitable animal model(s) which could illustrate an association linking obesity to LUTS. We examined the lower urinary tract function in an obesity-initiated MetS mouse model.

METHODS—Male C57BL/6N wild-type and obese B6.V-Lepob/J maintained on regular diet for 28 weeks were subjected to the assessment of body weight (BW), body length (BL), waist circumference (WC), body mass index (BMI), blood glucose (BG), plasma insulin (INS), plasma leptin (LEP), total cholesterol (CHO), free fatty acid (FFA) and measurement of urinary functions. Whole animal peritoneal and subcutaneous adipose tissue measurements as well as prostate and bladder volumes were analyzed by MRI followed by histological evaluation. These parameters were used to draw correlations between MetS and LUTS.

Correspondence to: Sanjay Gupta, Ph.D., Department of Urology, Case Western Reserve University & University Hospitals Case Medical Center, 10900 Euclid Avenue, Cleveland, Ohio 44106 Phone: (216) 368-6162, Fax: (216) 368-0213, sanjay.gupta@case.edu.

Disclosure: All authors disclose no financial or commercial conflict of interest.

RESULTS—Obesity parameters such as BW, WC, and BMI were significantly higher in B6.V-Lepob/J mice compared to C57BL/6N mice ($p<0.01$). Higher levels of total CHO and FFA were noted in B6.V-Lepob/J mice than C57BL/6N mice ($p<0.05$). These results were concurrent with frequency, lower average urine volume and other urinary voiding dysfunctions in B6.V-Lepob/J mice. MRI assessments demonstrate marked increase in body fat and prostate volume in these mice. Compared to C57BL/6N mice, histological analysis of the prostate from B6.V-Lepob/J mice showed increased proliferation, gland crowding and infiltration of immune cells in the stroma; whereas the bladder urothelium was slightly thicker and appears more proliferative in these mice. The regression and correlation analysis indicate that peritoneal fat ($R=0.853$; $p<0.02$), CHO ($R=0.729$; $p<0.001$), BG ($R=0.712$; $p<0.001$) and prostate volume ($R=0.706$; $p<0.023$) strongly correlate with LUTS whereas BMI, WC, INS, and FFA moderately correlate with the prevalence of bladder dysfunction.

CONCLUSION—Our results suggest that LUTS may be attributable in part to obesity and MetS. Validation of an *in vivo* model may lead to understand the underlying pathophysiological mechanisms of obesity-related LUTS in humans.

Keywords

metabolic syndrome; lower urinary tract symptoms; overactive bladder; prostate hyperplasia; urinary incontinence

INTRODUCTION

Over the years, obesity has emerged as one of the most prevalent chronic disorder worldwide and the second most preventable cause of death in the developed countries [1–4]. Approximately, 30% adults in the Western countries are considered obese characterized by lipid accumulation in both adipose and non-adipose tissues and accompanying endocrine aberration including insulin resistance and hypertension referred to as metabolic syndrome (MetS). In fact, MetS was proposed as an umbrella term to include subjects affected by cardiovascular and metabolic risk factors, such as visceral obesity, hypertension, hyperglycemia, low high-density lipoprotein cholesterol (HDL-C) and hypertriglyceridemia, in the effort to identify a diagnostic category able to predict cardiovascular-metabolic complications. The prevalence of MetS affects around 34–39% of the adult population in the United States [5].

Obesity, body size and composition has long been hypothesized to be related to lower urinary tract symptoms (LUTS) and benign prostatic hyperplasia (BPH) [3, 4]. A cluster of published evidence demonstrate that body weight, body mass index (BMI), and central obesity measured by waist circumference may increase the risk of BPH and LUTS [6–8]. Recent clinical studies suggested that MetS might be linked to BPH, LUTS, overactive bladder (OAB) and erectile dysfunction (ED) [3–5, 9, 10]. Although the associations potentially linking BPH/LUTS and MetS are not completely identified. Some studies suggest a feasible association between MetS and LUTS related to BPH, highlighting new targets for prevention and treatment of these disorders [11–13]. However, research into the link between MetS and these clinical conditions has been going on for a shorter period of time and limited in regions. Another major challenge is the choice of the appropriate

experimental model—an animal model suitable for studying the underlying mechanisms between obesity/MetS and LUTS. Although obesity and diabetes research is mostly conducted in mice on a C57BL/6 background, which facilitates diet-induced obesity and obesity-associated comorbidities, including glucose intolerance and hepatic steatosis [14, 15]; however, their susceptibility to diet-induced obesity and comorbid conditions always remains a major issue [16, 17].

This study was designed to provide the full metabolic characterization of B6.V-Lepob/J mice. We further aim to examine if there are correlations between the components of MetS and the parameters of urinary function measurements. Overall, our data address the question whether B6.V-Lepob/J mice can serve as a suitable translational model to study the link between obesity/MetS and LUTS. For the first time, we demonstrate that B6.V-Lepob/J mice on a C57BL/6 background are prone to the development of voiding dysfunction and symptoms of LUTS.

MATERIALS AND METHODS

Animals

Male C57BL/6N mice (n=20) and leptin-deficient obese male B6.V-Lepob/J mice (n=20) of eight weeks of age were purchased from Jackson Laboratories (Jackson Labs, Bar Harbor, ME) and maintained at 22–24°C under a 12:12-h light–dark cycle (lights on from 7:00 am to 19:00 pm). Individual mice were marked by ear punch for identification and *ad libitum* access to standard rodent chow and drinking water. All mice were maintained for 28 weeks and later euthanized. A series of parameter records were monitored during this period. Mice exhibiting higher blood glucose levels (≥400 mg/dl) were excluded from the study because they tend to lose weight with time and interfere in the study hypothesis considering the effects of obesity/MetS on LUTS, not diabetes. The bladder and prostate were harvested for histological examination. All experimental protocols were approved by the Case Western Reserve University Institutional Animal Care and Use Committee (IACUC #2012-0089).

Obesity parameters

Body weights were measured once a week. Waist circumferences, body lengths (nose to anus) were measured every two weeks. The BMI was then calculated as the body weight (g)/ body lengths $(cm)^2$. Food and water intake were recorded and measured monthly. Food intake was assessed by weighing the food in each cage dispenser, including the food that was spilled on the floor of the cage.

Blood glucose and glucose tolerance test

Blood glucose (BG) and glucose tolerance test (GTT) was performed following 16 h overnight fasting (17:00–9:00). BG was measured from the tail vein with an Accucheck® Aviva glucose meter (Roche Diagnostics, Indianapolis, IN) every two weeks. GTT was measured every four weeks with a 1g/kg dose of D-glucose intraperitoneal injection and blood was obtained from the tail for glucose measurement at time points 0, 30, 60, 90, 120 minutes. The area under the curve (AUC) for the GTT was calculated by the trapezoidal method [18].

Plasma insulin, leptin, cholesterol and fatty acid measurements

Plasma insulin levels (INS) and leptin were measured using a rat/mouse ELISA kit (Crystal Chem., Downers Grove, IL), and cholesterol levels were measured using an Amplex Red cholesterol assay kit (Molecular Probes, Invitrogen, Inc.); free fatty acids (FFA) were measured with a fatty acid quantitation kit (Sigma-Aldrich, Inc. MO, USA) following vendor's instruction.

Prostate volume measurements by MRI

MRI analysis was performed in 3–4 mice per group to evaluate the size of prostate enlargement at 14 weeks and 28 weeks of age. Anesthesia was induced on each mouse with 3% isoflurane, and maintained in 1–2% isoflurane in oxygen throughout the MRI procedure. Each mouse was placed on prone position inside a 30-cm, horizontal bore, 7T Bruker Biospec MRI Scanner (Bruker Incorporated, Billerica, MA). The animal's respiration rate (40–60 breaths/minute) and core body temperature (35+/− 2°C) were monitored and controlled continuously during the MRI scanning procedures using a small animal physiological monitoring system, supplied by Small Animal Instruments, Inc. (Stony Brook, NY). High resolution axial, fat-suppressed proton density-weighted MRI scans were acquired to obtain accurate delineation of the prostate from surrounding tissue (TR/TE = 5000/15 ms, matrx = 256 × 256, FOV = 3 × 3 cm, slice thickness = 0.7 mm). Prostate volumes were measured by manually selecting the prostate region using the scanner's host software.

Fat distribution by MRI

During the same imaging session above, adipose tissue bio-distribution at 14 weeks and 28 weeks of age was obtained using a previously described Relaxation Compensated Fat Fraction (RCFF) MRI technique [19]. The RCFF-MRI method uses multiple acquisitions to reliably separate fat and water tissue components in multiple coronal imaging slices over the entire mouse. The fat-only images are then used to calculate the total subcutaneous and peritoneal adipose tissue volumes for each animal.

Assessment of fluid consumption and urinary pattern measurement

Twenty-four-hour urination behavior was performed in a real time of 12-hour light, 12-hour dark cycle using mouse micturition chambers (Med Associates Inc., St. Alban, VT) once a month as previously described [20]. Briefly, 24 h before micturition measurement, solid food was removed from mice cages and replaced with lactose-free milk. This strategy substantially reduces the frequency and weight of the feces generated during testing and thereby prevents skewing of the urine collection and aberrations of data analysis. After 24 h live recording of urination behavior, a known volume of milk remaining in the drinking bottle, was recorded. The urinary frequencies were counted, the volumes per void were measured, and the total voiding volume was calculated.

Catheter implantation and conscious cystometrogram

Before euthanasia on 28 weeks, conscious cystometrogram (CMG) on a group of mice was performed to assess the voiding functions. Catheter implantation and CMG measurements

were performed as previously described [20]. Mice were anaesthetized with isofurane and a suprapubic bladder catheter was implanted. The bladder was exposed and a circular purse-string suture of 8–0 silk was placed on the bladder wall. A small incision was made in the bladder wall and the catheter (polyethylene-10 tubing with a flared tip) was implanted. A purse-string suture was tightened around the catheter. The catheter was tunneled subcutaneously and externalized at the back of the neck. The distal end of the tubing was sealed and the incisions were closed. CMG was performed 3 days after catheter implantation. Before starting cystometry, bladder was emptied via the third port. Continuous cystometry was performed by infusing 0.9% PBS into the bladder at a rate of 1.0 ml/h while bladder pressure was recorded. Data on at least 5 continuous and representative micturition cycles were collected. The mean was calculated to analyze CMG parameters, including peak pressure and inter-contraction interval, resting pressure, threshold pressure, peak pressure and voiding volume. In addition, functional bladder capacity (inter-contraction interval multiplied by the infusion rate) was calculated.

Histological examination

Bladder and prostate glands were fixed in 4% paraformaldehyde for routine histological examination. Paraffin-embedded prostate and bladder sections were cut and stained with hematoxylin and eosin.

Histological characterization of inflammation

H&E-stained slides were scored for volume of inflammation based on counts of infiltrating inflammatory cell aggregates, predominantly polymorphonuclear leukocytes in the mouse prostates as previously assessed [21].

Immunohistochemical analysis

Immunohistochemistry for proliferating cell nuclear antigen (PCNA) was performed on formalin-fixed, paraffin-embedded prostate and bladder tissue sections using a standard protocol as described previously using 3, 3′-diaminobenzidine and counterstaining with Mayer’s hematoxylin [22]. Sections were examined with an inverted Olympus BX51 microscope and images were acquired with Olympus MicroSuite™ Five Software (Soft Imaging System, Lakewood, CO).

Proliferation index

The proliferation index in the prostate and bladder of C57BL/6N and B6.V-Lepob/J mice were assessed in the proliferating region of the tissue using a standard protocol as described previously [23].

Statistical analysis

Data were analyzed using the SPSS 19.0 software package. Numerical variables that were normally distributed were expressed as Mean ± SEM and analyzed by independent sample t test. Pearson correlation analysis was used to evaluate the correlation of the data. A logistic regression was employed to relate the risk factors to the occurrence of the event. The voiding event frequency was considered as a dependent variable whereas all other significant

potential parameters were taken as independent variables. Univariate analysis was performed to obtain the odds ratio, 95% confidence interval and p value. The factors which presented statistical significance were considered to be the risk factors and would be included in the multivariate analysis. All statistical tests of hypotheses are two-sided and p value less than 0.05 were considered statistically significant.

RESULTS

The physical and metabolic characteristics of the B6.V-Lepob/J and C57BL/6N control mice of 28 weeks is shown in Table 1. Compared to control group, B6.V-Lepob/J mice showed statistically significant increase in BW ($P<0.001$), WC ($P<0.001$) and BMI ($p<0.001$) at each time point (Figure 1A–C). The B6.V-Lepob/J mice exhibited a marked increase in body weight compared to C57BL/6N at the end of 28 weeks (62.57 ± 3.96 g *versus* 30.92 ± 2.18 g; $p<0.001$). The increase in body weight gain in B6.V-Lepob/J mice correlated with increase in food intake, whereas no significant change was observed in fluid consumption compared to C57BL/6N mice (Supplemental Figure 1A & B). No significant differences were noted in the body length between B6.V-Lepob/J and C57BL/6N mice (data not show).

Next we measured the markers of MetS in these mice. As shown in figure 2A, fasting blood glucose (BG) level in B6.V-Lepob/J mice was almost ~200% of that noted in C57BL/6N between 8 to 12 weeks. The area under curve (AUC) of GTT showed that exacerbated glucose intolerance existed and a markedly blunted response to insulin stimulation at each time point (Figure 2B and Supplemental Figure 1C). We also confirmed the levels of insulin (INS), total cholesterol (CHO), free fatty acid (FFA) which were significantly elevated throughout the time period in B6.V-Lepob/J mice compared to the control mice (Figure 2C–E). The leptin levels measured at 28 weeks of age were significantly lower, as expected, in B6.V-Lepob/J mice compared to the C57BL/6N mice (Figure 2F). These results confirm that B6.V-Lepob/J mice exhibit components of MetS, including obesity, increased WC and BMI, higher fasting BG and INS levels, impaired glucose tolerance, hypocholesteremia (high-density cholesterol) and hyperlipidemia.

Next we use MRI to assess subcutaneous and peritoneal fat in B6.V-Lepob/J and C57BL/6N mice. An image acquisition followed by semiautomatic image segmentation algorithm was engaged to measure volumes of subcutaneous and peritoneal adipose tissue as previously described (Figure 3A) [19]. Both subcutaneous fat and peritoneal fat volume identified was significantly higher in B6.V-Lepob/J than C57BL/6N mice ($p<0.001$) (Figure 3B).

We next compared the voiding function in B6.V-Lepob/J and C57BL/6N mice by recording 24 h urination behavior and cystometrogram (CMG) measurement (Figure 4A–C). As shown in figure 4A, B6.V-Lepob/J mice exhibited a significantly increased voiding frequency compared to C57BL/6N control mice, whereas the average urine volume each void markedly decreased in B6.V-Lepob/J mice. Similar to 24 h urination behavior measurement, representative of CMG of 28 weeks in B6.V-Lepob/J mice before sacrifice demonstrate decrease in bladder capacity, voiding volume and inter-contraction interval time, compared to C57BL/6N mice (Table 1). However, the average resting pressure, threshold pressure, and peak micturition pressure increased in these mice (Table 1). These results suggest that the

B6.V-Lepob/J mice display symptoms of overactive bladder. Histopathological examination of the bladder urothelium from B6.V-Lepob/J mice appeared slightly thicker with scattered urothelial cells containing pigment granules, most likely lecithin, a product of cellular degradation, compared to C57BL/6N mice (Figure 4D-a). Furthermore, the urothelium of B6.V-Lepob/J mice compared to C57BL/6N mice exhibited higher proliferative index [19.77 ± 6.81 *versus* 18.27 ± 5.32; $p<0.02$] as evidenced by nuclear staining with PCNA (Figure 4-b), a 36-kDa auxiliary protein which plays an essential role in nucleic acid metabolism and is a component of replication and repair machinery [24].

Next we determined the prostate volume by MRI in B6.V-Lepob/J and C57BL/6N mice. The prostate volume was significantly higher in B6.V-Lepob/J mice compared to C57BL/6N mice imaged by MRI at 14 weeks and 28 weeks of age (Figure 5A & B). The prostate volume in C57BL/6N mice increased with time and varied from 21.0 ± 3.97 to 35.9 ± 13.8 mm^3 (Figure 5A-a-c & B); whereas a marked increase in prostate volume was noted in B6.V-Lepob/J mice which varied from 27.0 ± 6.74 to 67.5 ± 8.12 mm^3 ($p<0.001$) (Figure 5A-b-d & B). Histological examination of the prostate tissue of the B6.V-Lepob/J mouse, as compared to that of a C57BL/6N mouse, shows pronounced glandular cell enlargement. These glandular structures were markedly crowded and proliferative, virtually filled the central lumen of the gland, resulting in overall enlargement of the gland (Figure 5C-a). Staining with PCNA demonstrated increased proliferative index of the glandular epithelium of the B6.V-Lepob/J mice, compared to C57BL/6N mice [23.26 ± 7.43 *versus* 19.58 ± 5.52; $p<0.05$], which might also contribute in increased prostate size (Figure 5C-b). Features of malignancy, such as increased mitotic activity, nuclear overlapping, apoptosis, necrosis, or stromal invasion, were not identified up to 28 weeks in B6.V-Lepob/J mice. In the soft tissues adjacent to the prostatic glands, there is a prominent cellular infiltrate, composed of chronic inflammatory cells, most likely lymphocytes, plasma cells and macrophages. The volume of inflamed foci, qualitatively categorized as aggregates of infiltrating immune cells, were markedly higher in the prostates of B6.V-Lepob/J mouse as compared to that of a C57BL/6N mouse [11.16 ± 7.4 *versus* 3.66 ± 0.7; $p<0.001$], examined at ×100 magnification.

To understand the correlation of observed symptoms of MetS components towards increased voiding events during monitoring of urination behavior, we performed univariate and multivariate Pearson correlation analysis between the parameters identified in B6.V-Lepob/J and C57BL/6N mice. Voiding frequency has a positive moderate correlation with BW ($R=0.483$; $P<0.009$), BMI ($R=0.638$; $P<0.001$), WC ($R=0.469$; $P<0.012$), INS ($R=0.628$; $P<0.001$), FFA ($R=0.467$; $P<0.012$) and an association with peritoneal fat ($R=0.853$; $P<0.02$), total cholesterol ($R=0.729$; $P<0.001$), blood glucose ($R=0.712$; $P<0.001$), and prostate volume ($R=0.706$; $P<0.023$) respectively (Figure 6 and Supplemental Table 1). Four factors were found to be associated with increased voiding events in univariate analysis from B6.V-Lepob/J mice: BMI ($p=0.034$), BG ($p=0.001$), plasma insulin ($p=0.000$), cholesterol ($p=0.015$) (Table 2), whereas prostate volume and peritoneal fat were excluded as the limitation of sample size. Age ($p=0.069$), WC ($p=0.167$) and free fatty acid ($p=0.190$) were not significant prognostic indicators of increased voiding events in B6.V-Lepob/J mice (Table 2). Mathematically, BMI, blood glucose and total cholesterol fit into the final model to avoid multi-collinearity problem, and the result showed that only blood glucose (OR:

21.61; 95% CI: 1.84–253.30; p=0.014) was independently associated with voiding events (Table 2).

DISCUSSION

Obesity plays a key role in the pathogenesis of MetS and is strongly suggested to link with urinary voiding dysfunctions. Many studies indicate a close link between obesity and an increased risk of voiding dysfunctions, either BPH or LUTS [10, 25–27]. Similarly, several studies suggested that insulin resistance with secondary hyperinsulinemia is associated with prostatic enlargement [4, 28, 29]. Hyperinsulinemia is in turn associated with an increased sympathetic nervous system activity and may contribute to increase smooth muscle tone of the prostate, resulting in more severe LUTS independent of prostatic enlargement. Whereas not all studies support existence of positive association between MetS and voiding dysfunction, but we noticed that the available data with or without association between MetS and voiding dysfunctions derive from observational studies often geographically limited to a specific area or population. Thus, it's optimistic to explicitly evaluate these comparisons in an animal model, which are useful for gaining insight into pathophysiological mechanisms, for evaluating therapeutic interventions, and for screening novel therapeutic compounds and approaches in the management of LUTS. Due to controversy gap and limited literature on the animal research, we reasoned that it would be meaningful to conduct animal studies to define the relationship between MetS and voiding dysfunction.

The highlight of the current study, to our knowledge, is that we first used leptin-deficient B6.V-Lepob/J background strain mice to profile metabolic features such as weight gain, larger WC, body-mass accumulation, hyperinsulinemia, mild hyperglycemia, hypocholesteremia, hyperlipidemia, and define the characteristics of MetS-induced voiding dysfunctions. In addition, we conducted the correlation between obesity/MetS parameters and voiding dysfunction to further analyze critical risk factors. The pathogenesis of obesity-initiated metabolic syndrome-induced urinary voiding dysfunction are complicated. Previous studies have shown some evidence between MetS and voiding events in high-fat diet (HFD)-induced obese models [34–37]. Rabbits fed with HFD exhibited metabolic syndrome, as evidenced by hyperglycemia, glucose intolerance, increased serum triglycerides and cholesterol levels, increased mean arterial pressure and visceral fat tissue. These animals also developed bladder alterations and reduced bladder compliance [38, 39]. Another study showed that HFD-fed SAMP6 and AKR/J mice developed diet-induced obesity and type 2 diabetes concurrently with increased visceral adipose tissue, prostatic inflammation, prostatic and urethral tissue fibrosis, and urinary voiding dysfunction [40]. Our previous studies have shown that HFD intake increases oxidative stress and chronic inflammation in the prostate via activation of Stat-3 and NF-κB/p65 [41]. These observational studies demonstrate an association between MetS and increased risk of voiding dysfunctions that may be secondary to inflammation [11, 38–40]. In our study histopathological examination and MRI scan demonstrated increased prostate volume and inflammation which existed in B6.V-Lepob/J mouse prostate. The most striking histological changes in B6.V-Lepob/J mouse prostates at 28 weeks of age were stromal hyperplasia, gland crowding and their proliferation virtually filling the central lumen of the gland, resulting in overall enlargement

of the prostate. Whether high-caloric diet has greater propensity to generate prostate inflammation of HFD-induced MetS animal models need further investigation.

Different from the animal models consuming HFD, B6.V-Lepob/J mice could be much easier to mimic the obesity-induced metabolic syndrome phenotype, but also have a positive response on voiding dysfunctions via both 24 h urination behavior measurement and CMG, which represented increased voiding events, decreased inter-contraction interval and bladder capacity, and increased peak pressure with higher voiding events. In addition, histologic analysis of urothelium in bladder of B6.V-Lepob/J mice was slightly thicker and appears more proliferative along with scattered urothelial cells containing pigment granules, most likely lecithin (a product of cellular degradation) or less likely, hemosiderin (a product of red cell breakdown in the vicinity of the urothelial cells), an observation that requires further analysis. However, the harvested bladder at 28 weeks from B6.V-Lepob/J mice did not indicate any marked difference in their weights compared to C57BL/6N mice.

Studies have shown that the components of MetS can induce voiding dysfunction independent of their association [42]. The urinary dysfunction phenotype observed in leptin-deficient B6.V-Lepob/J mice may be a confounding effect of the components of MetS. For example, a study showed that that morbid obesity generate a higher cholinergic effect impairing regular breathing pattern through M2 muscarinic receptor expressed higher in cortex, midbrain, and cerebellum in B6.V-Lepob/J mice than C57BL/6N mice [43]. This indicated that cholinergic effect could be deregulated in B6.V-Lepob/J mice affecting normal physiological functions. Another study showed that rats fed with fructose present overactive bladder, along with up-regulation of M(2)- and M(3)-muscarinic receptors, may contribute to overactive bladder symptoms [44]. Clinical studies are awaited demonstrating whether these factors affect increased smooth muscle tone of the urinary tract and bladder over-activity.

As to the association between MetS components and voiding dysfunctions, clinical studies suggested that there is a close link exists. Previous research has demonstrated BMI [8, 27], body weight [40], and waist circumference [7] were positively associated with prostate volume and voiding dysfunctions. We use B6.V-Lepob/J mice to explore the effect of MetS components towards increased voiding frequency. We observed that BMI, BG, INS and CHO were identified to be the risk factors for voiding dysfunctions and only BG was independent in the final multivariate analysis. The founding accords with other clinical studies whereas BG was the only independent factor could be explained by the limitation of sample size. Moreover, subcutaneous and peritoneal fat assessed from MRI images were also excluded for the same reason. It might be possible that these factors may be significant and independent predictors of voiding functions with increase in sample size.

CONCLUSIONS

In summary, for the first time we demonstrate an effective animal model that mimic the features of MetS and urinary voiding dysfunction. The model recapitulates several epidemiologic and case-control studies of human populations that associate obesity/MetS with urinary voiding dysfunction. Further investigations are needed to confirm these findings

and to determine various molecular mechanism(s) which leads to physiologic changes in voiding behavior. Better understanding of urologic complications in animal models may further lead to test for pharmacological interventions important in the treatment of MetS or in the prevention of lower urinary tract abnormalities.

Supplementary Material

Refer to Web version on PubMed Central for supplementary material.

Acknowledgments

Financial Support: This work was supported by grants from United States Public Health Services P20DK090871 and 201306180078 from China Scholarship Council.

Abbreviations

LUTS	lower urinary tract symptoms
BPH	benign prostate hyperplasia
MetS	metabolic syndrome
OAB	overactive bladder
UI	urinary incontinence
BW	body weight
BL	body length
WC	waist circumference
BMI	body mass index
BG	blood glucose
INS	plasma insulin
LEP	plasma leptin
CHO	total cholesterol
FFA	free fatty acid
HDL-C	low high-density lipoprotein cholesterol
ED	erectile dysfunction
GTT	glucose tolerance test
RCFF	relaxation compensated fat fraction
MRI	magnetic resonance imaging
CMG	conscious cystometrogram

HFD high-fat diet

References

1. Alberti K, Eckel RH, Grundy SM, Zimmet PZ, Cleeman JI, Donato KA, et al. Harmonizing the Metabolic Syndrome A Joint Interim Statement of the International Diabetes Federation Task Force on Epidemiology and Prevention; National Heart, Lung, and Blood Institute; American Heart Association; World Heart Federation; International Atherosclerosis Society; and International Association for the Study of Obesity. Circulation. 2009; 120(16):1640–5. [PubMed: 19805654]
2. Freedland SJ, Terris MK, Presti JR, Amling CL, Kane CJ, Trock B, et al. Obesity and biochemical outcome following radical prostatectomy for organ confined disease with negative surgical margins. The Journal of urology. 2004; 172(2):520–4. [PubMed: 15247719]
3. Kasturi S, Russell S, McVary KT. Metabolic syndrome and lower urinary tract symptoms secondary to benign prostatic hyperplasia. Current Prostate Reports. 2006; 4(3):127–31.
4. Ozden C, Ozdal OL, Urgancioglu G, Koyuncu H, Gokkaya S, Memis A. The correlation between metabolic syndrome and prostatic growth in patients with benign prostatic hyperplasia. European urology. 2007; 51(1):199–206. [PubMed: 16806666]
5. Golden SH, Robinson KA, Saldanha I, Anton B, Ladenson PW. Prevalence and incidence of endocrine and metabolic disorders in the United States: a comprehensive review. The Journal of Clinical Endocrinology & Metabolism. 2009; 94(6):1853–78. [PubMed: 19494161]
6. Gacci M, Corona G, Salvi M, Vignozzi L, McVary KT, Kaplan SA, et al. A systematic review and meta-analysis on the use of phosphodiesterase 5 inhibitors alone or in combination with α-blockers for lower urinary tract symptoms due to benign prostatic hyperplasia. European urology. 2012; 61(5):994–1003. [PubMed: 22405510]
7. He Q, Wang H, Yue Z, Yang L, Tian J, Liu G, et al. Waist circumference and risk of lower urinary tract symptoms: a meta-analysis. The Aging Male. 2014; 17(4):223–9. [PubMed: 25295871]
8. Lee RK, Chung D, Chughtai B, Te AE, Kaplan SA. Central obesity as measured by waist circumference is predictive of severity of lower urinary tract symptoms. BJU international. 2012; 110(4):540–5. [PubMed: 22243806]
9. Kirby MG, Wagg A, Cardozo L, Chapple C, Castro-Diaz D, De Ridder D, et al. Overactive bladder: Is there a link to the metabolic syndrome in men? Neurourology and urodynamics. 2010; 29(8): 1360–4. [PubMed: 20589717]
10. Moul S, McVary KT. Lower urinary tract symptoms, obesity and the metabolic syndrome. Current opinion in urology. 2010; 20(1):7–12. [PubMed: 19904208]
11. Gacci M, Vignozzi L, Sebastianelli A, Salvi M, Giannessi C, De Nunzio C, et al. Metabolic syndrome and lower urinary tract symptoms: the role of inflammation. Prostate cancer and prostatic diseases. 2012; 16(1):101–6. [PubMed: 23165431]
12. Andersson KE, Nomiya M, Yamaguchi O. Chronic Pelvic Ischemia: Contribution to the Pathogenesis of Lower Urinary Tract Symptoms (LUTS): A New Target for Pharmacological Treatment? LUTS: Lower Urinary Tract Symptoms. 2015; 7(1):1–8. [PubMed: 26663644]
13. Besiroglu H, Otunctemur A, Ozbek E. The Relationship Between Metabolic Syndrome, Its Components, and Erectile Dysfunction: A Systematic Review and a Meta-Analysis of Observational Studies. J Sex Med. 2015; 12(6):1309–18. [PubMed: 25872648]
14. Bose M, Lambert JD, Ju J, Reuhl KR, Shapses SA, Yang CS. The major green tea polyphenol,(−)-epigallocatechin-3-gallate, inhibits obesity, metabolic syndrome, and fatty liver disease in high-fat–fed mice. The Journal of nutrition. 2008; 138(9):1677–83. [PubMed: 18716169]
15. Ueki K, Kondo T, Tseng Y-H, Kahn CR. Central role of suppressors of cytokine signaling proteins in hepatic steatosis, insulin resistance, and the metabolic syndrome in the mouse. Proceedings of the National Academy of Sciences of the United States of America. 2004; 101(28):10422–7. [PubMed: 15240880]
16. Gallou-Kabani C, Vigé A, Gross MS, Rabès JP, Boileau C, Larue-Achagiotis C, et al. C57BL/6J and A/J Mice Fed a High-Fat Diet Delineate Components of Metabolic Syndrome. Obesity. 2007; 15(8):1996–2005. [PubMed: 17712117]

17. Buettner R, Schölmerich J, Bollheimer LC. High-fat diets: Modeling the metabolic disorders of human obesity in rodents. Obesity. 2007; 15(4):798–808. [PubMed: 17426312]
18. Frassetto LA, Schloetter M, Mietus-Synder M, Morris R, Sebastian A. Metabolic and physiologic improvements from consuming a paleolithic, hunter-gatherer type diet. European journal of clinical nutrition. 2009; 63(8):947–55. [PubMed: 19209185]
19. Johnson DH, Narayan S, Wilson DL, Flask CA. Body composition analysis of obesity and hepatic steatosis in mice by relaxation compensated fat fraction (RCFF) MRI. Journal of Magnetic Resonance Imaging. 2012; 35(4):837–43. [PubMed: 22095745]
20. Liu G, Elrashidy RA, Xiao N, Kavran M, Huang Y, Tao M, Powell CT, Kim E, Sadeghi G, Mohamed HE, Daneshgari F. Bladder function in mice with inducible smooth muscle-specific deletion of the manganese superoxide dismutase gene. Am J Physiol Cell Physiol. 2015; 309(3):C169–78. [PubMed: 25948732]
21. Vykhovanets EV, Shukla S, MacLennan GT, Vykhovanets OV, Bodner DR, Gupta S. IL-1 beta-induced post-transition effect of NF-kappaB provides time-dependent wave of signals for initial phase of intrapostatic inflammation. Prostate. 2009; 69(6):633–43. [PubMed: 19170127]
22. Shukla S, Kanwal R, Shankar E, Datt M, Chance MR, Fu P, et al. Apigenin blocks IKKα activation and suppresses prostate cancer progression. Oncotarget. 2015; 6(31):31216–32. [PubMed: 26435478]
23. Elshazly MO, Abd El-Rahman SS, Morgan AM, Ali ME. The remedial efficacy of Spirulina platensis versus chromium-induced nephrotoxicity in male Sprague-Dawley rats. PLoS One. 2015; 10(6):e0126780. [PubMed: 26029926]
24. Jyostna P, Reddy MS, Ravikanth M, Narendra M, Dwarakanath CD. Expression of PCNA in oral gingival epithelium of aggressive and chronic periodontitis-A pilot study. Open J Stomatology. 2013; 3:112–117.
25. Kristal AR, Arnold KB, Schenk JM, Neuhouser ML, Weiss N, Goodman P, et al. Race/ethnicity, obesity, health related behaviors and the risk of symptomatic benign prostatic hyperplasia: results from the prostate cancer prevention trial. The Journal of urology. 2007; 177(4):1395–400. [PubMed: 17382740]
26. Parsons JK. Modifiable risk factors for benign prostatic hyperplasia and lower urinary tract symptoms: new approaches to old problems. The Journal of urology. 2007; 178(2):395–401. [PubMed: 17561143]
27. Xie L-P, Bai Y, Zhang X-Z, Zheng X-Y, Yao K-S, Xu L, et al. Obesity and benign prostatic enlargement: a large observational study in China. Urology. 2007; 69(4):680–4. [PubMed: 17445651]
28. Vikram A, Jena G, Ramarao P. Increased cell proliferation and contractility of prostate in insulin resistant rats: linking hyperinsulinemia with benign prostate hyperplasia. The Prostate. 2010; 70(1):79–89. [PubMed: 19790233]
29. Vikram A, Jena G, Ramarao P. Insulin-resistance and benign prostatic hyperplasia: the connection. European journal of pharmacology. 2010; 641(2):75–81. [PubMed: 20553919]
30. Corona G, Vignozzi L, Rastrelli G, Lotti F, Cipriani S, Maggi M. Benign prostatic hyperplasia: a new metabolic disease of the aging male and its correlation with sexual dysfunctions. Int J Endocrinol. 2014; 2014:329456. [PubMed: 24688539]
31. Comeglio P, Morelli A, Cellai I, Vignozzi L, Sarchielli E, Filippi S, et al. Opposite effects of tamoxifen on metabolic syndrome-induced bladder and prostate alterations: A role for GPR30/GPER? The Prostate. 2014; 74(1):10–28. [PubMed: 24037776]
32. Azadzoi KM, Tarcan T, Siroky MB, Krane RJ. Atherosclerosis-induced chronic ischemia causes bladder fibrosis and non-compliance in the rabbit. The Journal of urology. 1999; 161(5):1626–35. [PubMed: 10210430]
33. Morelli A, Comeglio P, Filippi S, Sarchielli E, Cellai I, Vignozzi L, et al. Testosterone and farnesoid X receptor agonist INT-747 counteract high fat diet-induced bladder alterations in a rabbit model of metabolic syndrome. The Journal of steroid biochemistry and molecular biology. 2012; 132(1):80–92. [PubMed: 22406511]

34. Gharaee-Kermani M, Rodriguez-Nieves JA, Mehra R, Vezina CA, Sarma AV, Macoska JA. Obesity-induced diabetes and lower urinary tract fibrosis promote urinary voiding dysfunction in a mouse model. The Prostate. 2013; 73(10):1123–33. [PubMed: 23532836]
35. Leiria LO, Silva FH, Davel AP, Alexandre EC, Calixto MC, De Nucci G, Mónica FZ, Antunes E. The soluble guanylyl cyclase activator BAY 60-2770 ameliorates overactive bladder in obese mice. J Urol. 2014; 191(2):539–47. [PubMed: 24050894]
36. Oberbach A, Jehmlich N, Schlichting N, Heinrich M, Lehmann S, Wirth H, et al. Molecular fingerprint of high fat diet induced urinary bladder metabolic dysfunction in a rat model. PLoS One. 2013; 8(6):e66636. [PubMed: 23826106]
37. Fan EW, Chen LJ, Cheng JT, Tong YC. Changes of urinary bladder contractility in high-fat diet-fed mice: the role of tumor necrosis factor-α. Int J Urol. 2014; 21(8):831–5. [PubMed: 24661252]
38. Cantiello F, Cicione A, Salonia A, Autorino R, Ucciero G, Tucci L, et al. Metabolic syndrome correlates with peri-urethral fibrosis secondary to chronic prostate inflammation: Evidence of a link in a cohort of patients undergoing radical prostatectomy. International Journal of Urology. 2014; 21(3):264–9. [PubMed: 23909794]
39. Vignozzi L, Rastrelli G, Corona G, Gacci M, Forti G, Maggi M. Benign prostatic hyperplasia: a new metabolic disease? Journal of endocrinological investigation. 2014; 37(4):313–22. [PubMed: 24458832]
40. Parsons JK, Sarma AV, McVary K, Wei JT. Obesity and benign prostatic hyperplasia: clinical connections, emerging etiological paradigms and future directions. The Journal of urology. 2013; 189(1):S102–S6. [PubMed: 23234610]
41. Shankar E, Vykhovanets EV, Vykhovanets OV, MacLennan GT, Singh R, Bhaskaran N, Shukla S, Gupta S. High-fat diet activates pro-inflammatory response in the prostate through association of Stat-3 and NF-κB. Prostate. 2012; 72(3):233–243. [PubMed: 21604287]
42. Mosli HA, Mosli HH, Bokhari AA. The effect of obesity and components of metabolic syndrome on urinary and sexual functions in Saudi men. Res Rep Urol. 2013; 5:91–7. [PubMed: 24400240]
43. Douglas CL, Bowman GN, Baghdoyan HA, Lydic R. C57BL/6J and B6.V-LEPOB mice differ in the cholinergic modulation of sleep and breathing. J Appl Physiol. 2005; 98(3):918–29. [PubMed: 15475596]
44. Lee WC, Chuang YC, Chiang PH, Chien CT, Yu HJ, Wu CC. Pathophysiological studies of overactive bladder and bladder motor dysfunction in a rat model of metabolic syndrome. J Urol. 2011; 186(1):318–25. [PubMed: 21600594]

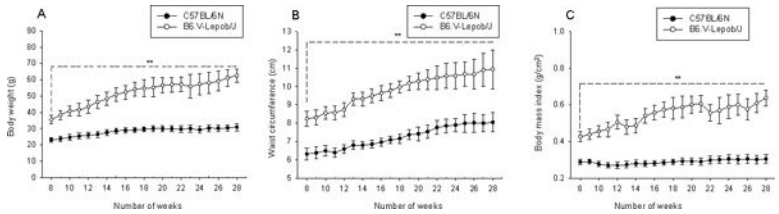

Figure 1.

Primary obesity parameters in C57BL/6N and B6.V-Lepob/J mice between 8–28 weeks. ***A***, body weight, ***B***, waist circumference, and ***C***, body mass index. A significant change has been observed in these parameters between the groups in time-dependent manner. Values represent Mean ± SEM, *p<0.05, **p<0.001, compared to C57BL/6 mice. Details are described in ‘materials and methods’ section.

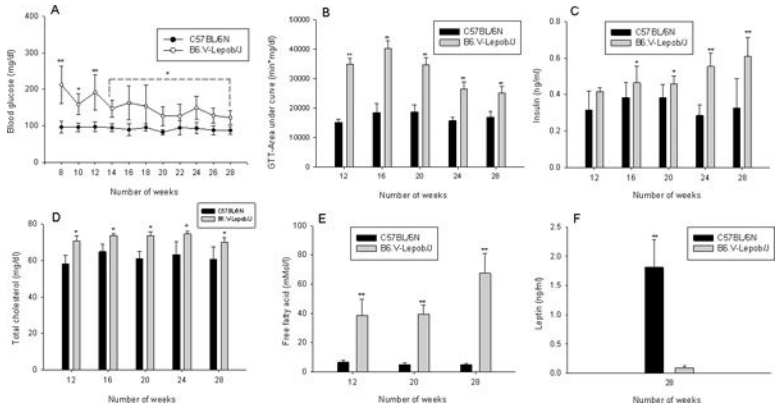

Figure 2.

Assessment of parameters of metabolic syndrome in C57BL/6N and B6.V-Lepob/J mice between 8–28 weeks. ***A***, blood glucose, ***B***, glucose tolerance test (GTT), ***C***, plasma insulin levels, ***D***, total cholesterol levels, ***E***, free fatty acid levels, and ***F***, leptin levels. A significant alteration in these parameters were noted between the groups in time-dependent manner. Values represent Mean ± SEM, *p<0.05, **p<0.001, compared to C57BL/6 mice. Details are described in ‘materials and methods’ section.

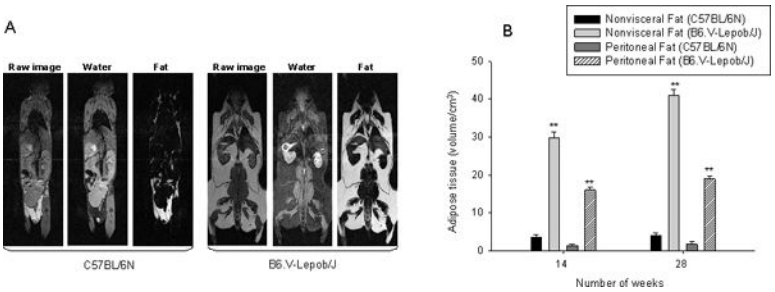

Figure 3.

Fat distribution assessment by MRI. ***A***, whole body raw MRI image, water and fat images in C57BL/6N and B6.V-Lepob/J mice was performed at 14 and 28 weeks. The RCFF technique was used for image segmentations and reconstruction for water and fat separation. The semiautomatic ratio image analysis program delineated the visceral adipose tissue (dark gray), subcutaneous adipose tissue (white), air (black), and other tissues. B, adipose tissue volume assessment in mice. ***B***, quantification of fat. Values represent Mean ± SEM, *p<0.05, **p<0.001, compared to C57BL/6 mice. Details are described in ‘materials and methods’ section.

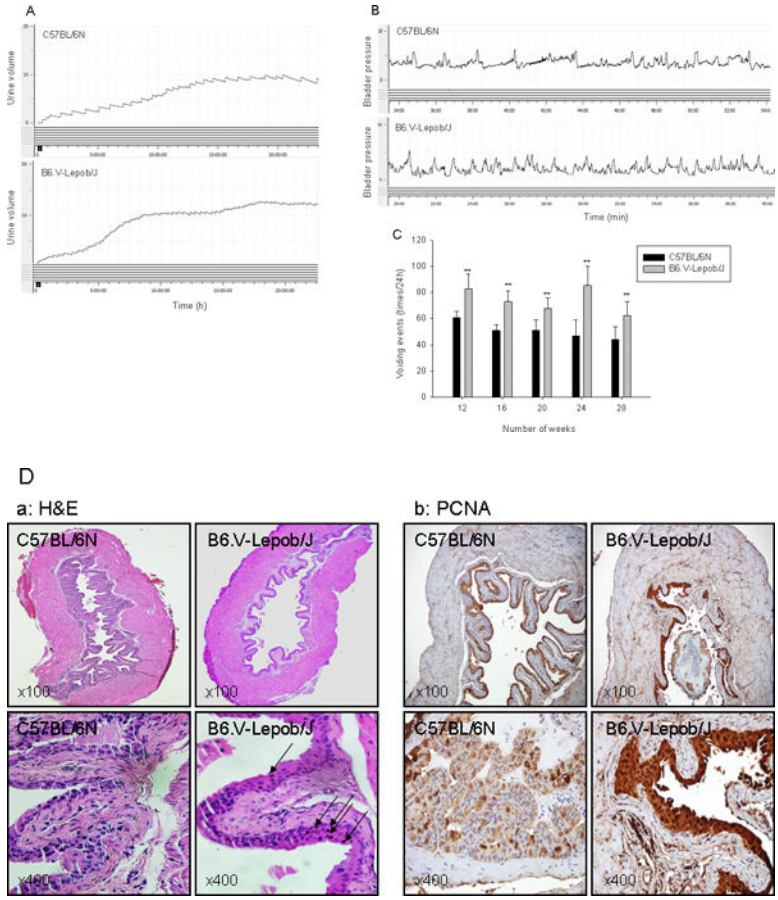

Figure 4.

Micturition, conscious cystometry monitoring and bladder histology and proliferation in C57BL/6N and B6.V-Lepob/J mice between 12–28 weeks. ***A***, typical voiding events at 24 h, ***B***, representative conscious cystometrogram, and ***C***, number of voiding events in 24 h. ***D-a***, representative image of H&E staining of the whole bladder at 28 weeks. ***D-b***, representative image of IHC staining of PCNA in the bladder urothelium at 28 weeks. A significant difference in micturition and voiding events were noted between the groups. Bladder of B6.V-Lepob/J mice, compared to C57BL/6N mice is slightly thicker and appears more proliferative along with scattered urothelial cells containing pigment granules, most likely lecithin (dark brown in color), as shown by arrows. Values represent Mean ± SEM, *p<0.05, **p<0.001, compared to C57BL/6 mice. Representative H&E and IHC staining photomicrograph of the mouse bladder (×100, and ×400 magnification). Details are described in ‘materials and methods’ section.

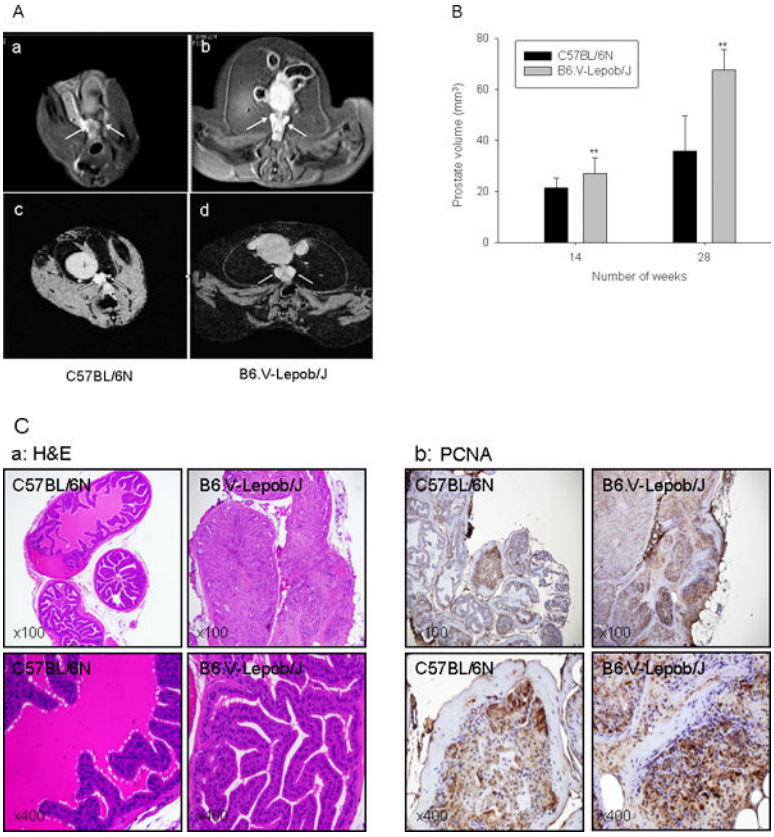

Figure 5.

Assessment of prostate volume by MRI, histology and proliferation in C57BL/6N and B6.V-Lepob/J mice at 14 and 28 weeks. ***A***, representative T1-weighted axial 2D gradient images of the mouse prostates a-c in C57BL/6N mice and b-d in B6.V-Lepob/J mice at 14 and 28 weeks. ***B***, prostate volume quantification. ***C-a***, representative image of H&E staining of the prostate gland at 28 weeks. ***C-b***, representative image of IHC staining of PCNA in the prostate at 28 weeks. A significant increase in the prostate volume was noted in B6.V-Lepob/J mice. Prostate of B6.V-Lepob/J mouse, as compared to that of a C57BL/6N mouse, shows pronounced glandular cell enlargement, markedly crowded and proliferative, virtually filled the central lumen of the gland, resulting in overall enlargement of the gland. Increase nuclear PCNA staining is noted in the prostate of B6.V-Lepob/J, compared to C57BL/6N mice. Values represent Mean ± SEM, *p<0.05, **p<0.001, compared to C57BL/6 mice. Representative H&E and IHC staining photomicrograph of the mouse prostate (×100, and ×400 magnification). Details are described in ‘materials and methods’ section.

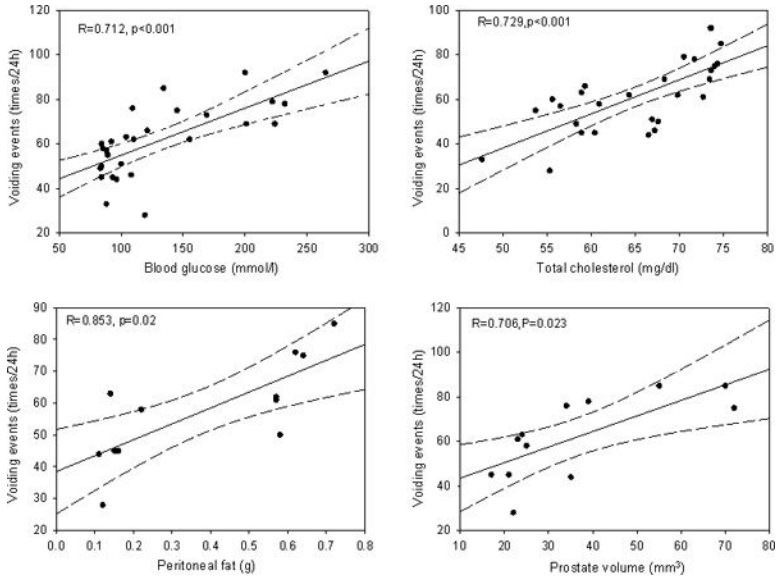

Figure 6.

Correlations of voiding events at 24 h to risk parameters: blood glucose, cholesterol, peritoneal fat, and prostate volume. Correlation coefficient (R) and p values are presented in each histogram.

Table 1

General information on bladder function, physical and metabolic parameters in 28 week old C57BL/6 and B6.V-Lepob/J mice.

	C57BL/6N mice	B6.V-Lepob/J mice
Obesity parameters		
Body weight (g)	30.92 ± 2.18*(20)*	62.57 ± 3.96 *(14)***
Waist circumference (cm)	8.05 ± 0.52*(20)*	10.94 ± 1.05 *(14)**
Body length (cm)	10.06 ± 0.21 *(20)*	10.05 ± 0.17 *(14)*
Body mass index (g/cm^2)	0.31 ± 0.02 *(20)*	0.62 ± 0.04 *(14)***
Water intake (ml/24h)	6.30 ± 0.31 *(8)*	8.10 ± 0.99 *(8)**
Plasma analysis		
Blood glucose (mg/dl)	87.47 ± 11.54 *(20)*	109.42 ± 22.21 *(14)**
Plasma insulin (ng/ml)	4.94 ± 0.04 *(6)*	67.47 ± 23.39 *(6)***
Cholesterol (mg/dl)	60.51 ± 7.00 (*9*)	69.8 ± 2.53 (5)*
Leptin (ng/ml)	1.51 ± 0.37 *(6)*	0.23 ± 0.14 *(6)***
Fatty acid (mmol/L)	0.36 ± 0.18 (*9*)	0.51 ± 0.24 (5)*
Twenty-four-hour Urination behavior		
Voiding events (times/24h)	40.75 ± 9.67 *(6)*	58.50 ± 12.61 *(6)***
Volume per void (ml/time)	0.60 ± 0.15 *(6)*	0.47 ± 0.10 *(6)***
Total voiding volume (ml/24h)	24.31 ± 3.82 *(6)*	28.41±5.57 *(6)**
Conscious Cystometry		
Average resting pressure (cmH_2O)	5.35 ± 0.49 *(3)*	11.12 ± 4.36 *(3)**
Threshold pressure (cmH_2O)	7.75 ± 1.11*(3*	20.72 ± 1.81 *(3)***
Peak micturition pressure (cmH_2O)	17.95 ± 1.18 *(3)*	28.59 ± 6.55 *(3)**
Bladder capacity (ml)	0.53 ± 0.17 *(3)*	0.34 ± 0.06 *(3)**
Voiding volume (ml)	0.36 ± 0.02 *(3)*	0.20 ± 0.02 *(3)**
Residual volume (ml)	0.12 ± 0.02 *(3)*	0.14 ± 0.07 *(3)*
Inter-contraction interval (sec)	300.50 ± 17.50 *(3)*	216.50 ± 97.64 *(3)**

Data represents the Mean ± SEM for 4–20 mice;

* p<0.05,

** p<0.01 vs C57BL/6N mice

Table 2

Risk factors for increasing voiding events in 28 week-old B6.VLepob/J mice

Risk factors	Univariate		Multivariate	
	Odds Ratio(95%CI)	*p* value	Odds Ratio	*p* value
Age(weeks)	4.40(0.89–21.78)	0.069	—	—
BMI(g/cm^2)	6.00(1.15—31.23)	0.034	2.68 (0.35–28.04)	0.305
WC(cm)	3.00(0.61—14.86)	0.167	—	—
Blood glucose (mg/dl)	33.00(3.18—342.26)	0.001	21.61 (1.84–253.30)	0.014
Plasma insulin (ng/ml)	35.00(4.20—291.98)	0.000	—	—
Cholesterol (mg/dl)	8.67(1.53—49.22)	0.015	3.14 (0.301–23.79)	0.378
Free fatty acid (mmol/L)	5.00(0.443—55.63)	0.190	—	—